Available online at www.sciencedirect.com
ScienceDirect
journal homepage: www.elsevier.com/locate/he

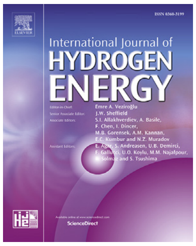

Numerical investigation of a high pressure hydrogen jet of 82 MPa with adaptive mesh refinement: Concentration and velocity distributions

Xinmeng Tang [a,*], *Edyta Dzieminska* [a], *Makoto Asahara* [b], *A. Koichi Hayashi* [a,c], *Nobuyuki Tsuboi* [d]

[a] *Department of Engineering and Applied Sciences, Faculty of Science and Technology, Sophia University, Yotsuya Campus 7-1 Kioi-cho, Chiyoda-ku, Tokyo, 102-8554, Japan*
[b] *Faculty of Engineering/Graduate School of Engineering, Gifu University, 1-1 Yanagido, Gifu, 501-1193, Japan*
[c] *Department of Mechanical Engineering, Aoyama Gakuin University, 5-10-1 Fuchinobe, Chuo-ku, Sagamihara, Kanagawa 229-8558, Japan*
[d] *Department of Mechanical and Control Engineering, Kyushu Institute of Technology, 1-1 Sensui-cho, Tobata-ku, Kitakyushu, Fukuoka 804-8550, Japan*

ARTICLE INFO

Article history:
Received 24 January 2018
Received in revised form
10 March 2018
Accepted 13 March 2018
Available online xxx

Keywords:
Underexpanded free jet
Hydrogen concentration
Adaptive mesh refinement
Numerical simulation
Turbulent oscillation

ABSTRACT

To investigate the safety properties of high-pressure hydrogen discharge or leakage, an under-expanded hydrogen jet flow with a storage pressure of 82 MPa from a small jet orifice with a diameter of 0.2 mm is studied by three-dimensional (3D) numerical calculations. The full 3D compressible Navier-Stokes equations are utilized in a domain with a size of about 3 × 3 × 6 m which is discretized by employing an adaptive mesh refinement (AMR) technology to reduce the number of grid cells. By AMR, the local mesh resolutions can narrowly cover the Taylor microscale l_T and direct numerical simulations (DNS) are performed. Both the instantaneous and mean hydrogen concentration distributions in the present jet are discussed. The instantaneous concentrations of hydrogen C_{H_2} on the axis presents significant turbulent pulsating oscillations. The centerline value of the intensity of concentration fluctuation $\widehat{\sigma}_{H_2}$ asymptotically comes to 0.23, which is in a good agreement with the existing experimental results. It substantiates the conclusion that the asymptotic centerline value of $\widehat{\sigma}_{H_2}$ is independent of jet density ratio. The probability distributions function (PDF) of instantaneous axial C_{H_2} agree approximately with the Gaussian distribution while skewing a little to the higher range. The time averaged hydrogen concentration $\overline{C}_{H_2}$ along the radial directions can also be described as a Gaussian distribution. The axial $\overline{C}_{H_2}$ of 82 MPa hydrogen jet tends to obey the distribution discipline approximated with $\overline{C}_{H_2} = 4200/(z/\theta)$ where z is the axial distance from the nozzle and θ is the effective ejection diameter, which is consistent with the experimental results. In addition, the hydrogen tip penetration Z_{tip} is found to be in a linear relationship with the square root of jet flow time $\sqrt{t}$. Meanwhile, the jet's velocity half-width L_{Vh} approximately gains an linear relation with z which can be expressed as $L_{Vh} = 0.09z$.

---

[*] *Corresponding author.*
E-mail addresses: simondonxq@gmail.com, shimon@pku.edu.cn (X. Tang).

https://doi.org/10.1016/j.ijhydene.2018.03.089
0360-3199/

Please cite this article in press as: Tang X, et al., Numerical investigation of a high pressure hydrogen jet of 82 MPa with adaptive mesh refinement: Concentration and velocity distributions, International Journal of Hydrogen Energy (2018), https://doi.org/10.1016/j.ijhydene.2018.03.089

Nomenclature

Roman Symbols

C_{H_2}	instantaneous mole concentrations of hydrogen (100%)
$\overline{C}_{H_2}$	time-averaged mole concentration of hydrogen (100%)
d	nozzle diameter (m)
d_n	notional nozzle diameter
dt, Dt	time step (s)
e	internal energy specific to per unit mass (J/kg)
$\mathbf{E}$, $\mathbf{F}$, $\mathbf{G}$	convection terms in generalized coordinates
$\mathbf{E}_v$, $\mathbf{F}_v$, $\mathbf{G}_v$	diffusion terms in generalized coordinates
FT_R	real part of the fast Fourier Transform
FT_{Im}	imaginary part of the fast Fourier Transform
J	Jacobian determinant
$\boldsymbol{J}$	Jacobian matrix
H	proportionality coefficient
H_m	height of Mach disk
l	integral scale
l_K	Kolmogorov microscale (m)
l_T	Taylor microscale (m)
Lv	adaptive mesh refinement level
L_{Vh}	velocity half-width (m)
M	molecular weights (kg/mol)
Ma	Mach number
$\dot{m}_{xi}$, $\dot{m}_{yi}$, $\dot{m}_{zi}$	components of mass diffusion flux in Cartesian coordinates (kg/(s·m^2))
$\dot{m}_{\xi i}$, $\dot{m}_{\eta i}$, $\dot{m}_{\zeta i}$	components of mass diffusion flux in generalized coordinates (kg/(s·m^2))
p	pressure (pa)
$\mathbf{Q}$	conservative solution vector
q_x, q_y, q_z	vector components of heat transfer flux in Cartesian coordinates (W/m^2)
q_ξ, q_η, q_ζ	vector components of heat transfer flux in generalized coordinates (W/m^2)
$\mathcal{R}$	the universal gas constant (8.3143 J/(mol·K))
R	gas constant for a specified gas
Re	Reynold number
$\mathbf{S}$	strain tensor
T	temperature (K)
t	time (s)
u, v, w	velocity components in Cartesian coordinates (m/s)
U, V, W	velocity components in generalized coordinates (m/s)
$\mathbf{V}$	velocity vector (m/s)
$\lVert\mathbf{V}\rVert$	magnitude of the velocity vector (m/s)
x, y, z	Cartesian coordinates (m)
Y	mass fraction of species (100%)
Z_{tip}	jet tip penetration (m)
Z	compressibility factor

Greek symbols

γ	specific heats ratio
Δ	local grid resolution (μm)
ξ, η, ζ	generalized coordinates
θ	effective ejection diameter (m)
λ_2	the second eigenvalue of tensor $\mathbf{S}^2+\boldsymbol{\Omega}^2$
μ	dynamic viscosity (Pa·s)
ρ	density (kg/m^3)
ρ_*	density of the sonic flow at the nozzle exit (kg/m^3)
σ_{H_2}	standard deviation of instantaneous axial hydrogen concentration
$\hat{\sigma}$	intensity of fluctuation
τ_{xx}, τ_{xy}, τ_{xz}	shear tensor components in the x direction in Cartesian generalized (N/m^2)
τ_{yx}, τ_{yy}, τ_{yz}	shear tensor components in the y direction in Cartesian generalized (N/m^2)
τ_{zx}, τ_{zy}, τ_{zz}	shear tensor components in the z direction in Cartesian generalized (N/m^2)
$\tau_{\xi\xi}$, $\tau_{\xi\eta}$, $\tau_{\xi\zeta}$	shear tensor components in the ξ direction in generalized (N/m^2)
$\tau_{\eta\xi}$, $\tau_{\eta\eta}$, $\tau_{\eta\zeta}$	shear tensor components in the η direction in generalized (N/m^2)
$\tau_{\zeta\xi}$, $\tau_{\zeta\eta}$, $\tau_{\zeta\zeta}$	shear tensor components in the ζ direction in generalized (N/m^2)
$\emptyset$	source term
$\boldsymbol{\Omega}$	vorticity tensor

Subscripts

a	ambient condition
air	air
e	nozzle exit
H_2	hydrogen
i	i-th species
s	stagnation condition
t	time
v	viscosity term
V	velocity

Introduction

Hydrogen is a promising fuel for the future considering that it is clean, efficient, easy to get and of a rather high energy density. Its acceptance and widespread utilization are close at hand due to both the increase of energy needs and the progress of technology. Meanwhile, due to its extremely low ignition energy, a wide range of flammability limits, and the high burning velocity, hydrogen-based energy systems need to be critically evaluated and studied to make sure that its utilization is of safety and to prevent the occurrence of accidents.

For the storage of hydrogen, usually it is of very high pressures for both volumetric and gravimetric efficiencies. In

Please cite this article in press as: Tang X, et al., Numerical investigation of a high pressure hydrogen jet of 82 MPa with adaptive mesh refinement: Concentration and velocity distributions, International Journal of Hydrogen Energy (2018), https://doi.org/10.1016/j.ijhydene.2018.03.089